

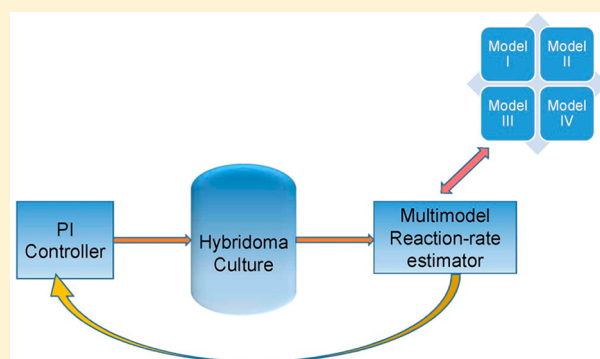
Simple Observer-Based Feedback Strategy for Controlling Fed-Batch Hybridoma Cultures

Federico A. Gorrini,[†] Silvina I. Biagiola,[†] José L. Figueroa,^{*,†} and Alain Vande Wouwer[‡]

[†]Instituto de Investigaciones en Ingeniería Eléctrica “Alfredo Desages,” UNS-CONICET, San Andrés 800, Palihue, 8000 Bahía Blanca, Argentina

[‡]Laboratoire d'Automatique, Faculté Polytechnique de Mons, 31 Boulevard Dolez, 7000 Mons, Belgium

ABSTRACT: Cultures of hybridoma cells in bioreactors are commonly used to produce monoclonal antibodies. As an alternative to nonlinear model predictive control, which has recently been applied successfully to optimize the process productivity, a simpler control approach is developed in the present study. This strategy is based on a classical PI controller and software sensors for the reaction rates, which exploit the particular structure of the dynamic model. The dynamic behavior of the process can indeed be subdivided into four operating zones, depending on the overflow metabolism of the hybridoma cells. In addition, robustness toward model uncertainties and measurement noise is investigated.



1. INTRODUCTION

Hybridoma cells are hybrid cells resulting from the fusion of a lymphocyte and a tumor cell. The interest in cultivating hybridoma cells lies in their capacity to produce specific monoclonal antibodies. For this reason, the pharmaceutical industry pays attention to the development of adequate bioprocesses, including the formulation of culture media and, more recently, on the feeding policy and possibly some form of automatic control strategy in order to improve performance and productivity.

In an attempt to describe the evolution of the cultures, different kinetic models were developed. One of the most recent and appropriate for process control is the dynamic model proposed by Amribt et al.¹ Cellular metabolism can follow two routes according to the available substrate concentration: the respiratory mode (below a threshold substrate) or the respiro-fermentative mode (with excess substrate) that generates inhibitory products (lactate and ammonia).

From a control point of view, the objective is to select an operation mode that maximizes the production of antibodies (or equivalently the production of biomass). To reach the optimum while avoiding the inhibitory regime, Dewasme et al.² resort to a closed loop optimization. Several optimizing control strategies dedicated to bioprocesses have been reported in the literature, including adaptive control, probing, robust, and predictive control.^{3–6} The use of nonlinear predictive control (NMPC)⁷ provides a natural and well-accepted structure for the formulation of optimal feedback control under constraints.

A simple and efficient approach to maintain the hybridoma culture in the optimum operation condition is the regulation of glucose and glutamine concentrations at their critical levels.^{5,8,9}

However, the sensors currently available for these types of measurements are expensive and delicate to use (in terms of acquisition, maintenance, and operational costs). For this reason, observers are frequently included in the control structure.

Dewasme et al.⁷ proposed a predictive controller based on the minimization of the deviation of the concentrations of glutamine and glucose from their critical values, thus maintaining the culture at the limit of the overflow metabolism.

For control implementation in the industry, the simplicity of the control strategy remains however an important constraint. Therefore, the objective of this study is to explore the possibility of designing a simple, yet robust, PID-like controller, based on the online estimation of the reaction rates. An original contribution is the development of a state estimation scheme which exploits the particular structure of the dynamic model. Moreover, the presence of parametric uncertainty is addressed.

This paper is organized as follows. In section 2, the mathematical model of hybridoma HB-S8¹ is briefly described, whereas section 3 is dedicated to control design. NMPC is first presented, as it will serve as a basis for comparison, and then attention is focused on the development of simple PI controllers for the reaction rates. Moreover, the design of an observer tailored to the application is detailed, based on a minimum variance unknown input observer.¹⁰ The performance achieved with the proposed feedback controller is

Received: August 15, 2017

Revised: December 1, 2017

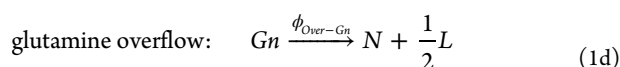
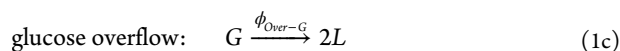
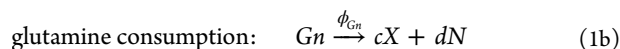
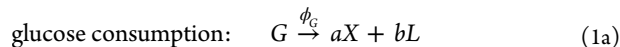
Accepted: December 2, 2017

Published: December 2, 2017

compared to the results obtained using NMPC.⁷ Conclusions and perspectives end this paper in section 4.

2. PROCESS MODEL

Hybridoma culture involves viable biomass (X_v) growth based on glucose and glutamine (G and G_n , respectively) consumption. A macroscopic model¹ based on the reduced metabolic network of HB-58 is the following:



where L and N represent lactate and ammonia, respectively. The symbols a , b , c , and d are the stoichiometric coefficients and ϕ_i ($i = G, G_n, \text{Over-G}, \text{Over-G}_n$) are the reaction rates given by the discontinuous overflow kinetic model recalling the bottleneck assumption¹¹ of

$$\phi_G = \min(\phi_{G1}, \phi_{G\max}) \quad (2a)$$

$$\phi_{G_n} = \min(\phi_{G_n1}, \phi_{G_n\max}) \quad (2b)$$

$$\phi_{\text{Over-G}} = \max(0, \phi_{G1} - \phi_{G\max}) \quad (2c)$$

$$\phi_{\text{Over-G}_n} = \max(0, \phi_{G_n1} - \phi_{G_n\max}) \quad (2d)$$

Each rate is the product of Monod-type specific consumption rates Γ_i ($i = G1, G_n1, G\max, G_n\max$) and the concentration of viable biomass X_v as in

$$\phi_{G1} = \Gamma_{G1}X_v = \mu_{G\max1} \frac{G}{K_G + G} \frac{G_n}{K_{G_n1} + G_n} X_v \quad (3a)$$

$$\phi_{G_n1} = \Gamma_{G_n1}X_v = \mu_{G_n\max1} \frac{G_n}{K_{G_n} + G_n} \frac{K_N}{K_N + N} X_v \quad (3b)$$

$$\phi_{G\max} = \Gamma_{G\max}X_v = \mu_{G\max2} X_v \quad (3c)$$

$$\phi_{G_n\max} = \Gamma_{G_n\max}X_v = \mu_{G_n\max2} X_v \quad (3d)$$

where $\mu_{i\max j}$ ($i = G, G_n; j = 1, 2$) are the maximum values of the specific kinetic rates and K_G , K_{G_n1} , and K_{G_n} are the half-saturation coefficients. K_N is the ammonia inhibition constant over the oxidation of glutamine.

This representation is based on the kinetic model contributed by Sonnleitner and Käppeli¹¹ which rests on the hypothesis that the strain metabolism is regulated by its respiratory capacity.

When substrate is in excess (for instance, when glucose concentration is above the critical level $G > G_{\text{crit}}$ and the consumption rate is $\Gamma_{G1} > \Gamma_{G\max}$), the cells produce lactate following the fermentative path and, therefore, the culture is in respiro-fermentative mode. On the other hand, when substrate becomes limiting (for instance, glucose concentration is below a critical level $G < G_{\text{crit}}$ and the substrate consumption rate $\Gamma_{G1} < \Gamma_{G\max}$) the culture is said to be in respirative regime.

Note that oxygen dynamics is not modeled because the system is assumed perfectly oxygenated and then the metabolic changes are essentially due to the substrate variation.

Mass balances on each component yield the following differential equations:

$$\frac{dX_v}{dt} = a\phi_G + c\phi_{G_n} - \mu_d X_v - DX_v \quad (4a)$$

$$\frac{dX_d}{dt} = \mu_d X_v - DX_d \quad (4b)$$

$$\frac{dG}{dt} = -\phi_G - m_G X_v - \phi_{\text{Over-G}} + D(G_{in} - G) \quad (4c)$$

$$\frac{dG_n}{dt} = -\phi_{G_n} - \phi_{\text{Over-G}_n} + D(G_{n\text{in}} - G_n) \quad (4d)$$

$$\frac{dL}{dt} = b\phi_G + 2\phi_{\text{Over-G}} + \frac{1}{2}\phi_{\text{Over-G}_n} - DL \quad (4e)$$

$$\frac{dN}{dt} = d\phi_{G_n} + \phi_{\text{Over-G}_n} - DN \quad (4f)$$

$$\frac{dV}{dt} = DV \quad (4g)$$

where m_G is the maintenance coefficient of glucose (note that maintenance on glutamine is not considered as it is negligible compared to oxidation and overflow), V is the reactor volume, $D = F_{in}/V$ is the dilution rate, F_{in} is the feed rate, and G_{in} and $G_{n\text{in}}$ are the substrate concentrations in the feed medium. X_d stands for the dead biomass concentration and the kinetics μ_d is

$$\mu_d = \mu_{\text{dmax}} \frac{K_{Gd}}{K_{Gd} + G} \frac{K_{G_{nd}}}{K_{G_{nd}} + G_n} \quad (5)$$

The substrate inhibition terms in eq 5 mean that cell death is limited if there is enough glucose and glutamine in the bioreactor.

The model parameter values used in this study are those reported by Dewasme et al.⁷ and are listed in Table 1. The relative uncertainties on the parameters were estimated based on the Fisher information matrix and will be used in the sequel of this paper to assess the robustness of the proposed control strategy (with the exception of the last parameter whose value is quite uncertain but fixed for the purpose of this study with a more reasonable coefficient of variation of 30%).

Table 1. Model Parameter Values and Uncertainties⁷

	values	coefficients of variation
$\mu_{G\max1}$	1.0006 h ⁻¹	8.23%
$\mu_{G\max2}$	0.0283 h ⁻¹	5.71%
$\mu_{G_n\max1}$	0.1992 h ⁻¹	7.92%
$\mu_{G_n\max2}$	0.0203 h ⁻¹	3.64%
μ_{dmax}	0.0111 h ⁻¹	10.73%
K_G	23.235 mM	11.99%
K_{G_n}	0.0004 mM	18.21%
K_N	0.9931 mM	11.86%
K_{G_n1}	0.0005 mM	21.81%
a	1.1462×10^5 cells/mM of G	6.46%
b	1.2939 mM of L/mM of G _n	6.90%
c	0.1186×10^5 cells/mM of G _n	21.52%
d	0.3000 mM of N/mM of G _n	6.39%
m_G	0.0367 mM mL/10 ⁵ cells	1.80%
K_{Gd}	2.4888 mM	25.60%
$K_{G_{nd}}$	0.0020 mM	117.19%

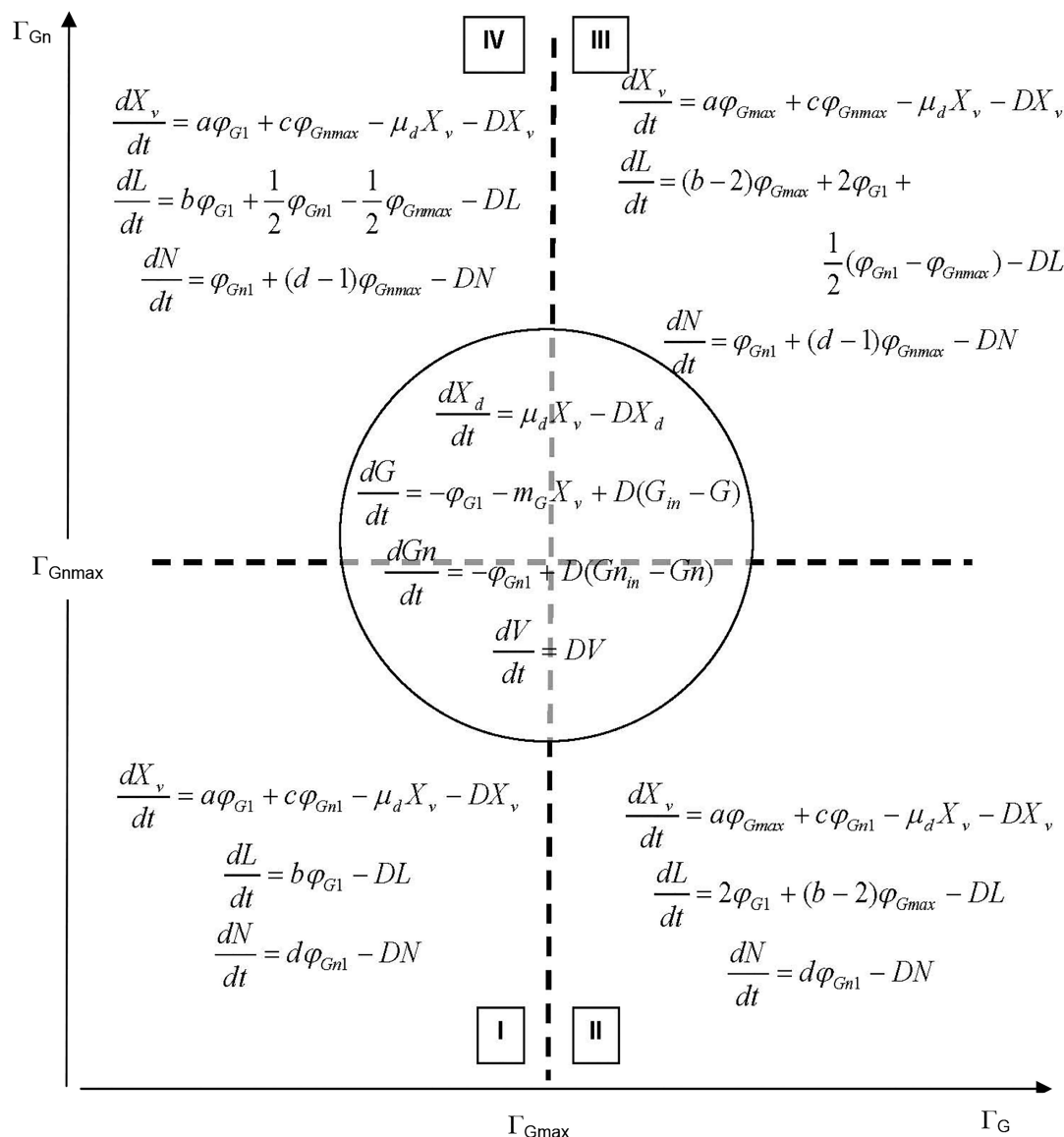


Figure 1. Possible regions of operation.

During the experiments the inlets G_{in} and Gn_{in} remained at 15 and 4 nM, respectively. Those values are also considered in this work.

Depending on the time evolution of substrate consumption (see eqs 2a–2d), the cell culture may pass through any of the four possible operating regions (I–IV), which are depicted in Figure 1. The dynamical behavior varies from one region to the other, as described by eqs 4a, 4e, and 4f.

3. PROCESS CONTROL

3.1. Background: Nonlinear Predictive Control Strategy. Dewasme et al.² performed a comparison of several objective functions in order to achieve optimum cell productivity in the bioreactor. They concluded that the two best candidate functions are those that measure the deviations of glutamine and glucose from their critical values. This means that the culture should be maintained at the limit of overflow, and the following cost function is proposed at time t_k :

$$\begin{aligned}\phi(t_k) &= \sum_{i=1}^p (\Gamma_{G1,k+i} - \Gamma_{Gmax,k+i})^2 \\ &+ \sum_{i=1}^p (\Gamma_{Gn1,k+i} - \Gamma_{Gnmax,k+i})^2\end{aligned}\quad (6)$$

This function is defined over a prediction horizon p , and it must be minimized to determine future values of the dilution rate. The control movements are penalized to avoid excessive changes in the feed. This leads to the following modified cost function

$$\psi(t_k) = \phi(t_k) + \gamma \sum_{i=1}^m (F_{in,k+i-1} - F_{in,k+i-1}^-)^2\quad (7)$$

where m is the control horizon ($m < p$), F_{in} is the manipulated variable, and F_{in}^- is the inlet value obtained in a previous optimization calculation. The manipulated variable can be calculated solving the following problem:

$$\begin{aligned}
 & \min_u \psi(t_k) \\
 & s. t. \dot{x} = f(x, u, \theta), t \in [t_k, t_{k+p}] \\
 & x_L \leq x \leq x_U \\
 & u_L \leq u \leq u_U \\
 & \Delta u_L \leq \Delta u_{j-1} \leq \Delta u_U, j = 1, \dots, m \\
 & \Delta u_j = 0, j > m
 \end{aligned} \quad (8)$$

Identical initial conditions were considered in all simulations: $X_v(0) = 1.85 \times 10^5$ cells/mL, $X_d(0) = 0.25 \times 10^5$ cells/mL, $G(0) = 17.17$ mM, $G_n(0) = 2.41$ mM, $L(0) = 0.36$ mM, $N(0) = 0.23$ mM, and $V(0) = 0.35$ L.

In a first step, the process controlled with NMPC is simulated, and for this purpose, the nominal model is used. In Figure 2 the six species concentrations are depicted (eqs 2a–2c) as well as the kinetics evolutions (eq 2d).

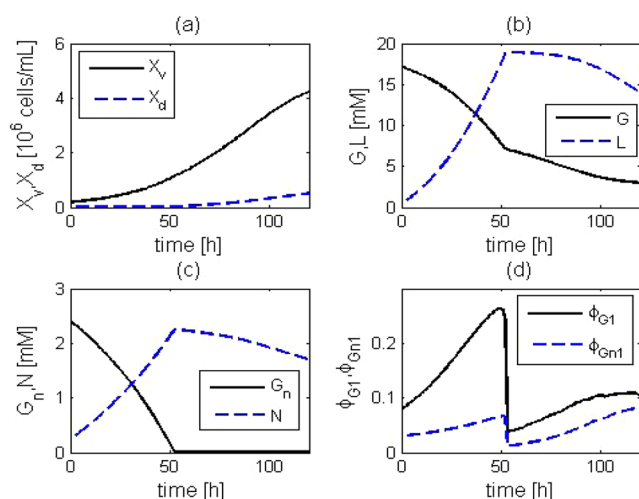


Figure 2. Nominal case: concentrations and kinetics evolutions with NMPC.

In a second step, robustness analysis is performed. For this purpose, the optimal profile of the manipulated variable (calculated for the nominal situation) is applied to 2^{16} process realizations corresponding to all of the possible combinations of the extreme values of 16 model parameters in Table 1. From this large number of cases, only those that contribute to form the envelopes (i.e., the upper and lower bounds) of biomass trajectories are selected, e.g., 17 cases out of 2^{16} .

The same simulation conditions as in Dewasme et al.⁷ are considered: the controller parameters are set to $p = 6$, $m = 3$, and $\gamma = 10^5$, and a culture time of $t_f = 120$ h is selected. Figure 3 shows (red dots) the evolution of X_v for each of these 17 cases under the NMPC strategy. This computational study shows the effect of applying the control law that minimizes the objective function [eq 7] (calculated with the nominal model), to each of the worst cases without information on the actual (internal) state of the process.

Another important point to consider is the potential benefits of state estimators. To evaluate this, NMPC is now calculated under the assumption of complete knowledge of each of the worst cases. The results obtained are shown with blue circles in Figure 3.

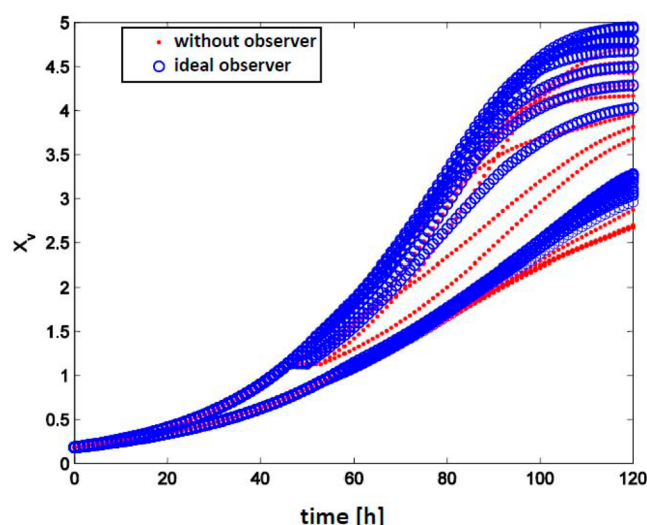


Figure 3. Robustness analysis of NMPC: variation in the achievable final biomass concentration due to parameter uncertainty.

In this case, a better performance is achieved than the one obtained with the nominal model. While this is not a realistic scenario, it serves as an upper bound performance which could be achieved if an ideal observer would be included in the algorithm. To distinguish both situations, we call these two cases as without observer and with ideal observer. To establish quantitative differences between the control schemes it is necessary to define numerical indices. As the aim of the process is to achieve maximum biomass production, we propose as a measure of achieved performance the average between the worst and the best cases and, as a measure of robustness, the deviation between the extreme cases and this value. Table 2 contains the numerical results for these cases.

Table 2. Controller Performance Indices

strategy	performance	robustness
NMPC without observer	3.6892	1.0208
NMPC + ideal observer	3.9550	0.9917
PI without observer	3.7539	1.2598
PI with ideal observer	4.4009	1.3318
PI with real observer	4.0744	1.0783

3.2. Simple Feedback Controller. A simple feedback controller is now developed based on the error signal:

$$e(t) = \Gamma_G(t) - \Gamma_{G_{\max}}(t) \quad (9)$$

where $\Gamma_G = \min(\Gamma_{G1}, \Gamma_{G_{\max}})$. Note that this definition of the error is in line with the objective function defined in eq 6.⁷ As it will be shown, this single error signal allows very good results to be achieved, with the great advantage of transforming the control problem into a SISO one.

Therefore, the PI control law is defined as follows:

$$F_m(t) = K_c \left(e(t) + \frac{1}{T_i} \int_0^t e(t) dt \right) \quad (10)$$

where K_c and T_i are the well-known PI controller design parameters. In the sequel, the controller settings are selected as $K_c = 0.8$ and $T_i = 0.5$. Figure 4 shows the viable biomass and

the control action for the nominal plant, while Figure 5 shows the signals $\Gamma_{G_{\max}}$ and Γ_{G_1} .

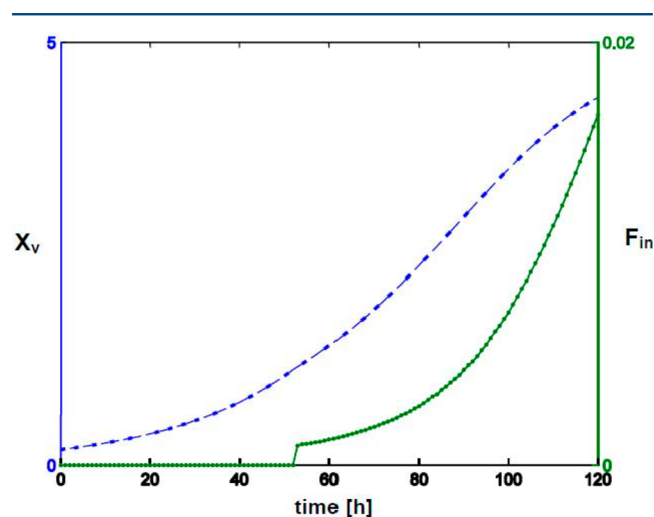


Figure 4. Viable biomass and manipulated variable evolution with PI control.

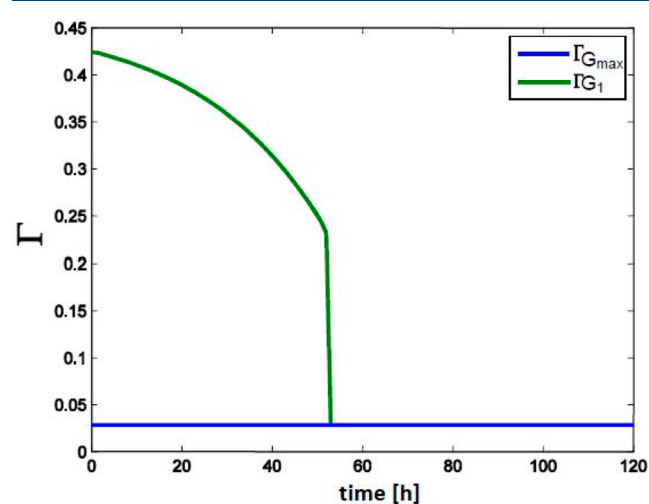


Figure 5. Γ_{G_1} and $\Gamma_{G_{\max}}$ with PI control.

Figure 6 illustrates the evolution of X_v for each worst-case scenario when the control move is calculated using the nominal model (red dots) and with a perfect knowledge of the internal

state (ideal observer) of the system (blue circles). In analogy with Figure 3, all of the realizations that contribute to form the envelope of the family of possible biomass trajectories are considered. Note that the performance achieved with the PI controller is comparable to that obtained with NMPC. Table 2 quantifies the depicted results. The PI controller is less robust than NMPC, but with the inclusion of an ideal observer, it could outperform NMPC.

3.3. Observer-Based Output-Feedback Control Strategy. 3.3.1. Statement of the Problem.

The underlying idea is to provide the control algorithm reliable information about the internal state of the process, particularly, an estimation of those reaction rates that cannot be calculated because they depend on unmeasured variables. For this purpose, the available model of the process described in section 2 is essential (see Figure 1).

Based on the available sensors, it is assumed that the states X_v , L , and N are measured and the volume V can be calculated.

In order to have a more appropriate mathematical process representation to estimate the unknown kinetics of interest (i.e., φ_{G_1} and $\varphi_{G_{n1}}$), the following description is proposed:

$$\text{sector 1: } \begin{bmatrix} \dot{L} \\ \dot{N} \end{bmatrix} = \begin{bmatrix} -D & 0 \\ 0 & -D \end{bmatrix} \begin{bmatrix} L \\ N \end{bmatrix} + \begin{bmatrix} b & 0 \\ 0 & d \end{bmatrix} \begin{bmatrix} \varphi_{G_1} \\ \varphi_{G_{n1}} \end{bmatrix} \quad (11)$$

$$\text{sector 2: } \begin{bmatrix} \dot{L} \\ \dot{N} \end{bmatrix} = \begin{bmatrix} -D & 0 \\ 0 & -D \end{bmatrix} \begin{bmatrix} L \\ N \end{bmatrix} + \begin{bmatrix} 2 & 0 \\ 0 & d \end{bmatrix} \begin{bmatrix} \varphi_{G_1} \\ \varphi_{G_{n1}} \end{bmatrix} + \begin{bmatrix} (b-2)\varphi_{G_{\max}} \\ 0 \end{bmatrix} \quad (12)$$

$$\text{sector 3: } \begin{bmatrix} \dot{L} \\ \dot{N} \end{bmatrix} = \begin{bmatrix} -D & 0 \\ 0 & -D \end{bmatrix} \begin{bmatrix} L \\ N \end{bmatrix} + \begin{bmatrix} 2 & 1/2 \\ 0 & 1 \end{bmatrix} \begin{bmatrix} \varphi_{G_1} \\ \varphi_{G_{n1}} \end{bmatrix} + \begin{bmatrix} (b-2)\varphi_{G_{\max}} - 1/2\varphi_{G_{n\max}} \\ (d-1)\varphi_{G_{n\max}} \end{bmatrix} \quad (13)$$

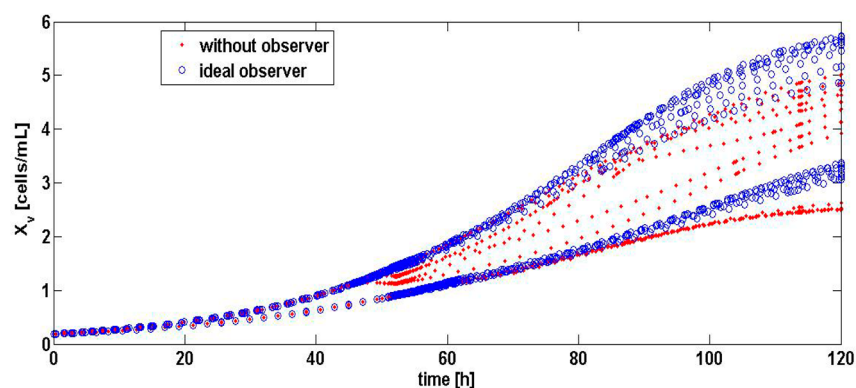


Figure 6. Robustness analysis of PI controller: variation in the achievable final biomass concentration due to parameter uncertainty.

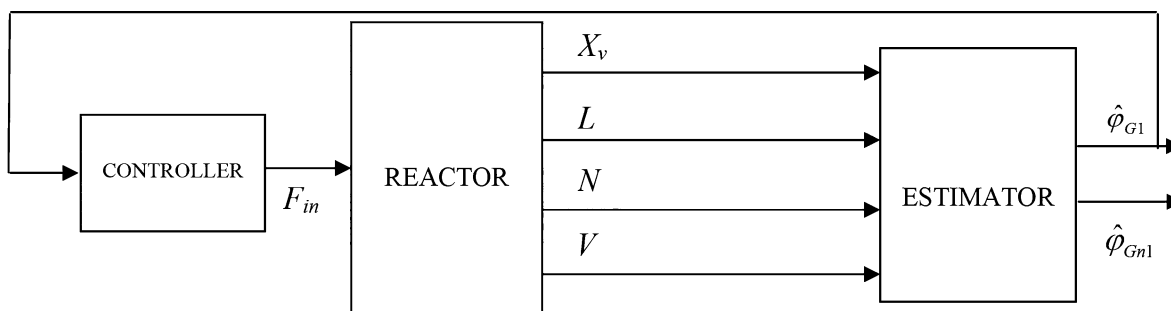


Figure 7. Overall scheme of the controller-estimator structure.

sector 4:

$$\begin{bmatrix} \dot{L} \\ \dot{N} \end{bmatrix} = \begin{bmatrix} -D & 0 \\ 0 & -D \end{bmatrix} \begin{bmatrix} L \\ N \end{bmatrix} + \begin{bmatrix} b & 1/2 \\ 0 & 1 \end{bmatrix} \begin{bmatrix} \varphi_{G1} \\ \varphi_{Gn1} \end{bmatrix} + \begin{bmatrix} -1/2\varphi_{Gnmax} \\ (d-1)\varphi_{Gnmax} \end{bmatrix} \quad (14)$$

Therefore, a global state space model can be written for each sector

$$\dot{x} = Ax + B_s u + C_s \quad (15)$$

The state vector contains the lactate and ammonia concentrations, which can be measured online and could be used to build an unknown input estimator of the following form:

$$\dot{\hat{x}} = A\hat{x} + B_s \hat{u} + C_s \quad (16)$$

$$y = x \quad (17)$$

where $\hat{x}(t)$ denotes the state estimate, y the measured states, and \hat{u} the input estimate. Matrices A , B_s , and C_s have a given structure in each sector, with $s = \{1, 2, 3, 4\}$ indicating the sector.

3.3.2. Reaction-Rate Estimator. As data acquisition in the hybridoma culture depends on sensors of different nature, the admissible sampling frequency will vary from one physical variable to another. In fact, while biomass can be measured in continuous time using a plunging probe, the concentrations of other components can be measured by various ways but with some sort of sampling (automatic or manual), so that sampling time could increase up to 30 min.

To take into consideration the practical limitation due to sampling, a tailored estimation strategy should be selected. The overall scheme of the proposed controller-estimator structure is shown in Figure 7.

To cope with the bioprocess characteristics, i.e., uncertain kinetics and multirate sampling, an approach of both state and input estimation is proposed. This means that the kinetics φ_{G1} and φ_{Gn1} are considered as external inputs instead of states-dependent functions. Even though this is not true, this strategy allows “decoupling” the complete model [eqs 4a–4g] and to use a reduced model with only two states (L and N). In this scenario, the extended Kalman filter (EKF) appears as an appropriate tool to address the problem.¹² As the unknown kinetics are treated as unmeasured fictitious inputs, it is possible to modify the conventional EKF algorithm in order to estimate the states as well as the inputs. The idea of input estimation was dealt with by Gillijns and De Moor,¹⁰ addressing the problem of simultaneously estimating the state and the input of a linear

discrete-time system in the presence of process/measurement noises.

An extension of this unknown input observer to nonlinear continuous-time model and discrete-time measurements can be accomplished using linearization around the estimated trajectory in a way similar to the EKF.¹³ This extension is not required here as the model [eq 15] appears in linear form.

The following estimation algorithm consists in three steps. The first one is prediction:

I-Time update

$$\dot{\hat{x}} = A\hat{x} + B_s u_{[klk]} + C_s \quad (18)$$

$$\dot{P} = A(t)P + PA^T(t) + Q \quad (19)$$

$$\hat{x}_{[k+1]k} = \hat{x}((k+1)T) \quad (20)$$

$$P_{[k+1]k} = P((k+1)T) \quad (21)$$

The time update is achieved using the original continuous-time model of the hybridoma culture [eqs 11–14], starting from the last corrected state. Equation 18 is based on the model of the process given in eq 15, where A depends on F_{in} and V , and C_s depends on X_v . It is assumed that viable biomass and reactor volume are continuous measurements. Equation 19 allows the calculation of the covariance matrix evolution.

The design parameters of the estimator are selected as $Q = I_2$ and the covariance initialization condition is set to $P(0) = 0.15^2 I_2$, where I_2 represents the identity matrix of dimension 2×2 .

As regards matrix Q , it is associated with model uncertainty which affects the prediction of the future state of the system. It is generally related to unmodeled dynamics and parameter uncertainties which are frequently represented as process noise. In the context of the present hybridoma cells culture, the parameter Q should also take account of the possible sector change (see Figure 1), which can be interpreted as modeling uncertainty. The selection of Q equal to the identity matrix implies a quite uncertain model. With respect to the term C_s in eq 16, it can be calculated through its corresponding sector model in eqs 11–14. The only source of error in the evaluation of C_s could be due to parameter uncertainty or sector commutation. However, the estimator can cope with unmeasured disturbances and/or model parameter uncertainty provided this is taken into account in the setting of Q .¹⁴

Practical observation shows that sector commutation has not drastic consequences for the estimator algorithm, i.e., the model used by the estimator only differs from the real one for very few samples.

An additional step with respect to the classical EKF algorithm is the estimation of the unmeasurable kinetics:

II-Estimation of the unknown kinetics

$$\begin{aligned}
 \bar{R}_{[k+1]} &= CP_{[k+1|k]}C^T + R \\
 \bar{M}_{[k+1]} &= (F_s^T \bar{R}_{[k+1]}^{-1} F_s)^{-1} F_s^T \bar{R}_{[k+1]}^{-1} \\
 u_{[klk+1]} &= \bar{M}_{[k+1]}(y_{[k+1]} - C\hat{x}_{[k+1|k]}) \\
 P_{u[kl|k+1]} &= (F_s^T \bar{R}_{[k+1]}^{-1} F_s)^{-1}
 \end{aligned} \quad (22)$$

where $F_s = CB_s$ and $C = I_2$ as the whole state vector is measured (see eq 17). Note that the approach in [eq 22] provides the necessary information to accomplish optimization of biomass production without the knowledge of the unmeasured states G and Gn .

The design parameter R is $\text{diag}\{(0.2)^2; (0.02)^2\}$ which takes the noise level in the measured variables L and N into account. The measurement noise is generally interpreted as the inaccuracy introduced by the sensor itself. However, in the context of the present application, the measurement noise is mainly interpreted as a fictitious measurement error related to the mismatch between the real value of the continuous-time signal and its last sampled value. In order to select the value for the matrix R , the changes in both variables, L and N , were analyzed each time a new sample was acquired. The diagonal elements of the covariance matrix R were chosen in accordance with the observed “commutation” jumps of L and N . In this way, the disturbance caused by the noncontinuous measurement process is interpreted as an equivalent measurement noise.

The third and last step consists in the measurement update:

$$\begin{aligned}
 \hat{x}_{[k+1|k+1]} &= \hat{x}_{[k+1|k]} + B\hat{u}_{[klk+1]} \\
 \bar{L}_{[k+1]} &= \bar{P}_{[k+1|k]}C^T\bar{R}_{[k+1]}^{-1} \\
 \bar{P}_{[k+1|k+1]} &= \bar{P}_{[k+1|k]} + BP_{u[kl|k+1]}B^T - BP_{u[kl|k+1]}F_s^T\bar{L}_{[k+1]}^T \\
 &\quad - \bar{L}_{[k+1]}F_sP_{u[kl|k+1]}B^T \\
 \hat{x}_{[k+1|k+1]} &= \hat{x}_{[k+1|k+1]} + \bar{L}_{[k+1]}(y_{[k+1]} - C\hat{x}_{[k+1|k+1]}) \\
 P_{[k+1|k+1]} &= \bar{P}_{[k+1|k+1]} - \bar{L}_{[k+1]}(\bar{R} - F_sP_{u[kl|k+1]}F_s^T)\bar{L}_{[k+1]}^T
 \end{aligned} \quad (23)$$

Figure 8 illustrates how the complete estimation algorithm works.

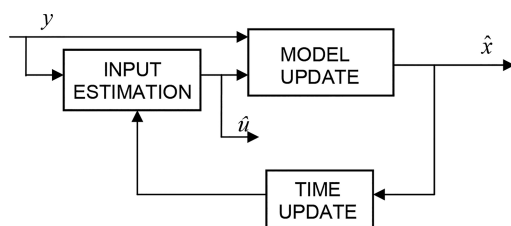


Figure 8. Block diagram of the overall observer structure.

3.3.3. Observability Analysis. An ad-hoc observability analysis can be performed. As described in eq 15, the dynamics relating $x = [L \ N]^T$ is given by

$$\dot{x} = Ax + B_s u + C_s$$

with $u = [\varphi_{G1} \ \varphi_{Gn1}]^T$. This could be interpreted as the following extended system whose states are to be estimated, provided the assumption of slowly time-varying kinetics (i.e., negligible du/dt). This is quite reasonable for this process as, from the kinetics data depicted in Figure 2, numerical approximations of time derivatives are those shown in Figure 9. Consequently

$$\begin{aligned}
 \dot{x}_{\text{ext}} &= \begin{bmatrix} -D & 0 & b_{s11} & b_{s12} \\ 0 & -D & 0 & b_{s22} \\ 0 & 0 & 0 & 0 \\ 0 & 0 & 0 & 0 \end{bmatrix} x_{\text{ext}} + \begin{bmatrix} c_{s1} \\ c_{s2} \\ 0 \\ 0 \end{bmatrix} \\
 y &= \begin{bmatrix} 1 & 0 & 0 & 0 \\ 0 & 1 & 0 & 0 \end{bmatrix} x_{\text{ext}}
 \end{aligned} \quad (24)$$

with $x_{\text{ext}} = [x, u]^T$.

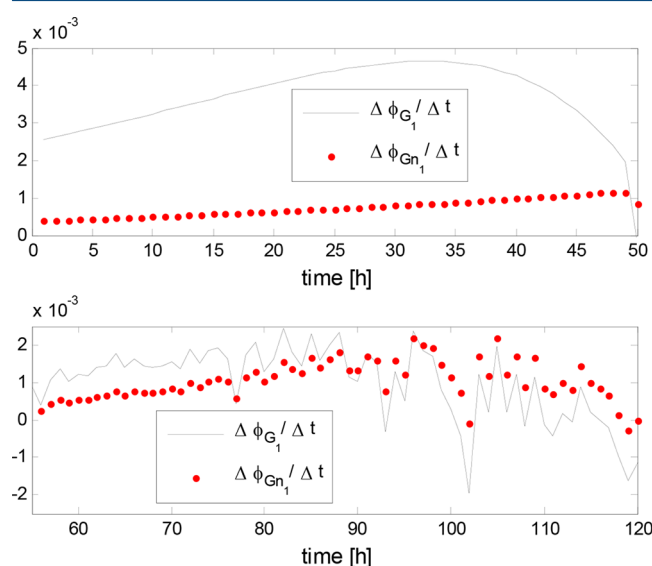


Figure 9. Numerical time-derivatives of the kinetics depicted in Figure 2.

The previous expression can be written in the following condensed form

$$\begin{aligned}
 \dot{x}_{\text{ext}}(t) &= f(x_{\text{ext}}(t), D(t)), \quad x_{\text{ext}}(0) = x_{\text{ext}0} \\
 y(t) &= Cx_{\text{ext}}(t)
 \end{aligned} \quad (25)$$

where $x_{\text{ext}} \in \mathcal{R}^n$, ($n = 4$). A system of the form in eq 25 is said to be observable¹⁵ on $X_{\text{ext}} \times \Delta^0 \times \dots \times \Delta^{(n-1)}$ if

$$\begin{aligned}
 \text{rank} \left\{ \frac{\partial}{\partial x_{\text{ext}}} \begin{bmatrix} y \\ \frac{dy}{dt} \\ \vdots \\ \frac{d^{n-1}y}{dt^{n-1}} \end{bmatrix} \right\} &= n, \forall (x_{\text{ext}}, D^0, \dots, D^{(n-1)}) \\
 &\in \bar{X} \times \Delta^0 \times \dots \times \Delta^{(n-1)}
 \end{aligned}$$

For the bioprocess under consideration

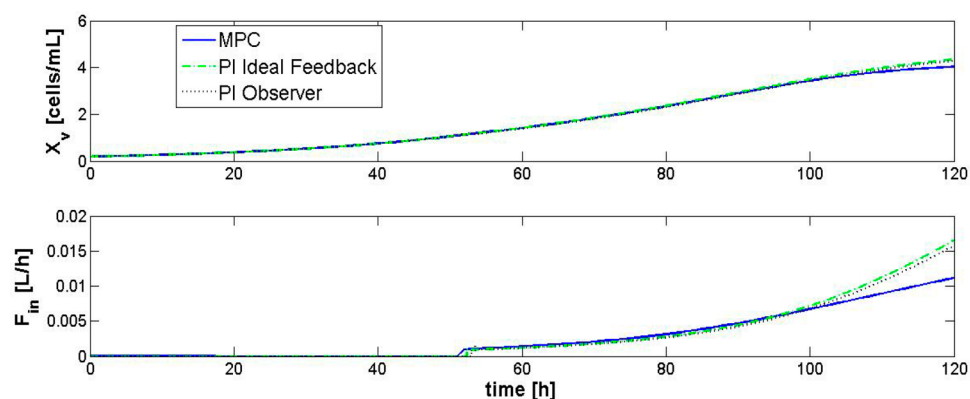


Figure 10. Comparison of NMPC and PI + estimator: evolution of biomass (X_v) and input flow (F_{in}).

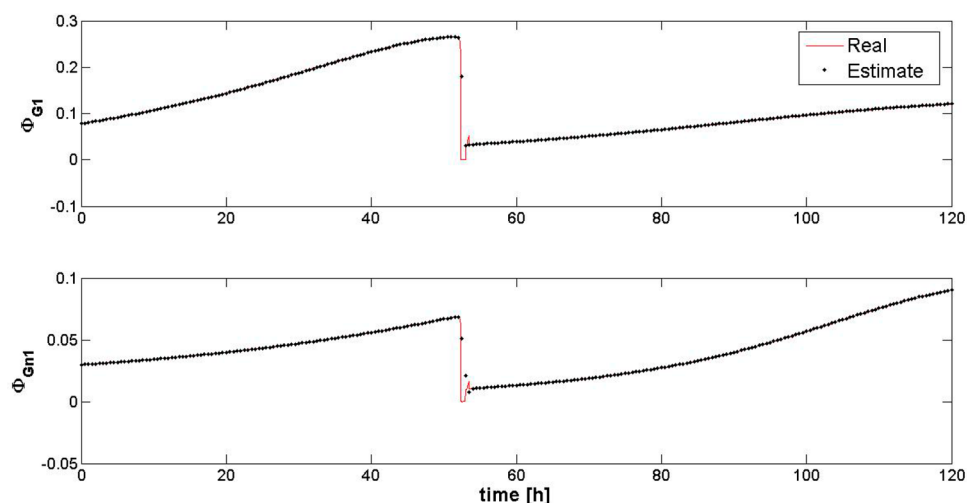


Figure 11. Estimation of the reaction rates ϕ_{G_1} and $\phi_{G_{n1}}$.

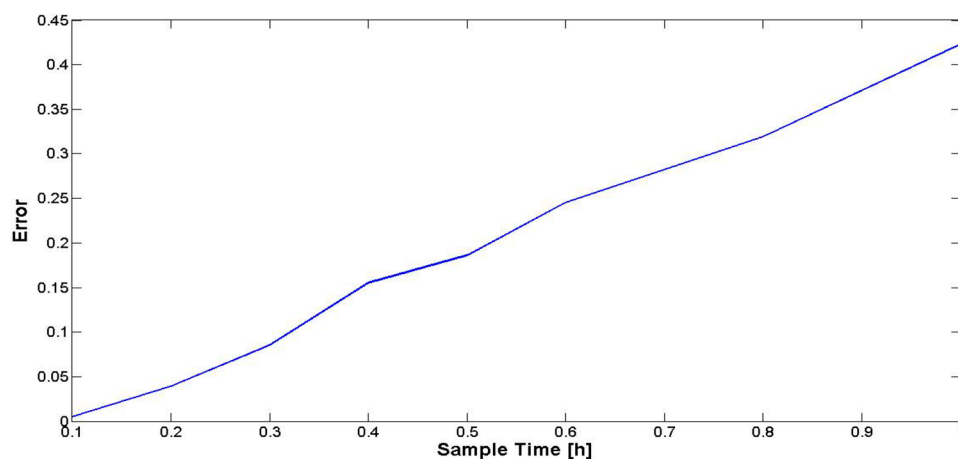


Figure 12. Estimation error.

$$\frac{\partial}{\partial x_{ext}} \begin{bmatrix} L \\ \frac{dL}{dt} \\ N \\ \frac{dN}{dt} \end{bmatrix} = \begin{bmatrix} 1 & 0 & 0 & 0 \\ -D & 0 & b_{s11} & b_{s12} \\ 0 & 1 & 0 & 0 \\ 0 & -D & 0 & b_{s22} \end{bmatrix}$$

Consequently, rank = 4 because b_{s11} and b_{s22} are never null regardless of the sector (see eqs 11–14).

3.3.4. Performance Assessment. For comparison purposes, the performances achieved with three control strategies (NMPC, PI with ideal feedback, and PI with state estimation) are depicted in Figure 10. From the above figure it can be noted that an improvement of 7.85% in biomass production can be achieved with ideal PI with respect to MPC-based production. Note that the observer-based PI strategy does not differ much

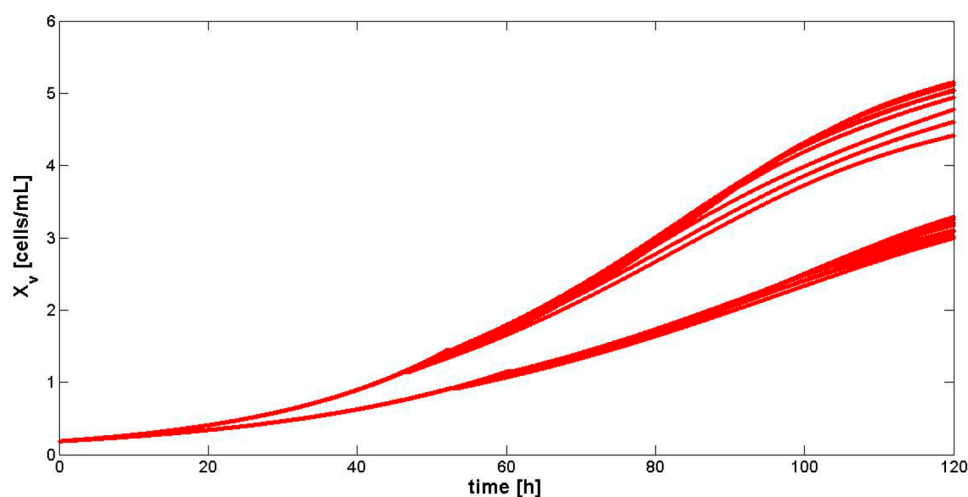


Figure 13. Robustness analysis—viable biomass.

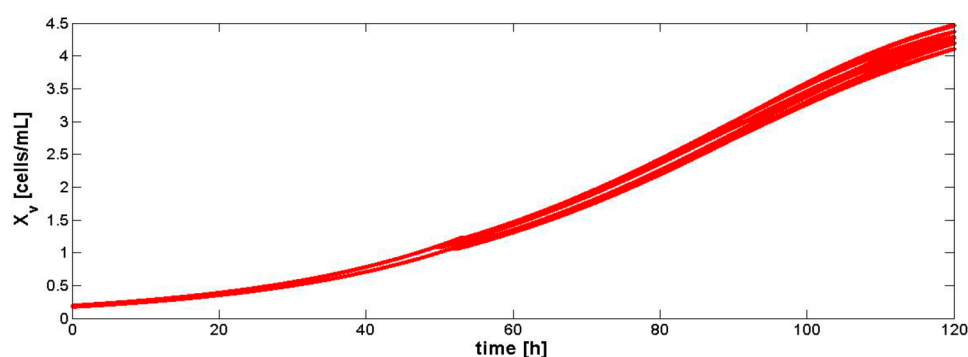


Figure 14. Sensitivity analysis for errors in the initial values of the states-viable biomass.

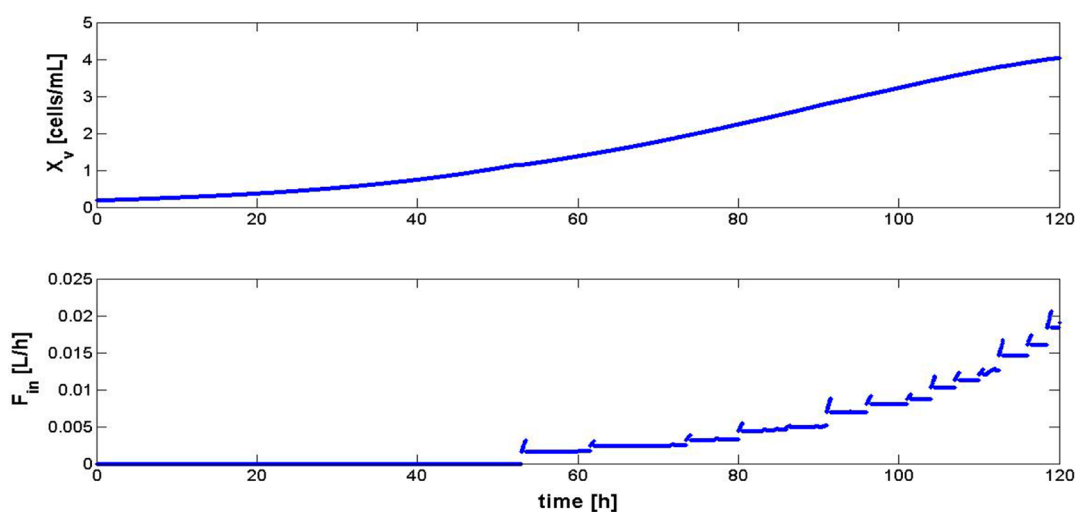


Figure 15. Viable biomass and manipulated variable (under additive measurement noise scenario).

from the ideal situation (i.e., with known kinetics). Although this production improvement could sound relative small, the high-added value of the product validates such moderate increase. It should be highlighted that to achieve such improvement with PI control, an augmented final input flow (F_{in}) is necessary (see the below picture in Figure 10). Indeed, for $t = 120$ h the required F_{in} is 47.32% larger than the input flow calculated by the model predictive controller. Figure 11 illustrates the estimated and the actual values for φ_{G1} and φ_{Gn1} ,

respectively. The rapid convergence of the estimation errors toward zero can be observed. Moreover, both kinetics show slow changes inside each sector, and when sector commutation occurs, the estimates follow quite well the actual values. This behavior, i.e., the slow time-variation kinetics, validates the assumption made in eq 24 and provides favorable conditions for carrying out the online estimation coupled with the process feedback control.

The dependence of the estimation error on the sampling time of the measured variables is now analyzed. Figure 12 illustrates the results. The error is computed as the sum of the squared errors between the estimated variable and the actual value. It is observed that the error increases almost linearly with the sampling time. In order to draw this figure, 1200 data were used to compute each error value regardless of the measurement sampling time.

To accomplish a robustness analysis of the proposed scheme, different simulations are performed for the worst control cases (i.e., 17 realizations) and worst estimation cases (i.e., 10 cases). The simulation results are depicted in Figure 13. The average value of the biomass at the end of the batch is 4.0744 cells/mL, and its deviation is 1.0783. Note that the results agree with those obtained in Figure 6, i.e., the observer-based PI control performance (Figure 13) is situated between those of the ideal PI control (circles in Figure 6) and the observer-free situation (dots in Figure 6). As expected, ideal PI control outperforms biomass productivity both in the lower and in the upper bounds cases.

Additional simulations are performed to check the robustness of the observer based controller against possible error in the initial values of the states. For this purpose, bounds of $\pm 5\%$ around the nominal initial values are considered. Figure 14 presents the results that show the low sensitivity of the control scheme with respect to the initial estimation error.

Finally, an additional test was performed to evaluate what happens when the estimation is based on noisy measurements, e.g., a viable biomass measurement corrupted with an additive noise signal with zero mean and a covariance equal to $(0.03X_v)_s^2$, where the subscript "s" stands for stationary state. For the measured variables N and L , the covariance values were assumed to be $(0.03N_s)^2$ and $(0.03L_s)^2$, respectively. The results are depicted in Figure 15. From comparison with Figure 6, it is apparent that the presence of measurement noise implies a more discontinuous control action and slightly decreases the maximum attainable biomass concentration. Nevertheless, the performance of the controller is still acceptable.

4. CONCLUSIONS

The nonlinear characteristic and the presence of discontinuities in the mathematical model of fed-batch hybridoma HB-58 cultures impose the design of a dedicated control strategy.

In order to increase hybridoma fed-batch culture productivity an ad hoc control algorithm is designed using a mathematical model of the process under the assumption of overflow metabolism.

The main contribution of this work is the development of a new control strategy that combines feedback controllers with estimation of unknown kinetics whose values are required by the control algorithm. The proposed approach makes an intensive use of the mathematical model of the system under study. The recognition of four distinct dynamics regions allows reformulating the complete model as four simple structures. The algorithm performance is tested in the presence of parameter uncertainty as well as additive measurement noise. Satisfactory results are obtained in both situations. The achieved performance is comparable with that obtained with NMPC to track a trajectory following the boundary of two metabolic pathways.

This control strategy has mainly the advantage of avoiding online numerical optimization, which is computationally

expensive and is not guaranteed to always converge whatever the situation.

As regards future work, this procedure could be tested on other bioprocesses whose dynamical behavior can be described with several simple models each of them valid for a limited region of the overall domain. This strategy appears as an appealing method for reducing the order of the model handled by the state estimator. Moreover, the proposed observer-based controller structure can be tested for multirate measurements of the different measurable species for improvement assessment compared to previous works. Finally, the proposed global structure could be altered to replace the PI controller by a MPC one, while the estimator as well as the region-based modeling are maintained.

AUTHOR INFORMATION

Corresponding Author

*E-mail: figueroa@uns.edu.ar.

ORCID

José L. Figueroa: 0000-0003-3956-9985

Notes

The authors declare no competing financial interest.

ACKNOWLEDGMENTS

The authors gratefully acknowledge funding support from CONICET-FNRS Bilateral Cooperation Programme Level 1 under the project "Observer and control design for biological systems with modelling uncertainties" (CONICET Res. D. No. 002935/15), CONICET (PIP 112-201101-01005), and Universidad Nacional del Sur (PGI 24/K077).

REFERENCES

- (1) Amribt, Z.; Niu, H.; Bogaerts, P. Macroscopic modelling of overflow metabolism and model based optimization of hybridoma cell fed-batch cultures. *Biochem. Eng. J.* **2013**, *70*, 196–209.
- (2) Dewasme, L.; Amribt, Z.; Santos, L. O.; Hantson, A. L.; Bogaerts, P.; Vande Wouwer, A. Hybridoma cell culture optimization using nonlinear model predictive control. *12th IFAC Symposium on Computer Applications in Biotechnology*, Mumbai, India, 16–18 December, 2013.
- (3) Pomerleau, Y. Modélisation et commande d'un procédé fed-batch de culture des levures à pain. Ph.D. Thesis; Département de génie chimique, Université de Montréal: Montréal, 1990.
- (4) Akesson, M. Probing control of glucose feeding in *Escherichia coli* cultivations. Ph.D. Thesis; Lund Institute of Technology: Sweden, 1999.
- (5) Dewasme, L.; Richelle, A.; Dehottay, P.; Georges, P.; Remy, M.; Bogaerts, P.; Vande Wouwer, A. Linear robust control of *S. cerevisiae* fed-batch cultures at different scales. *Biochem. Eng. J.* **2010**, *53*, 26–37.
- (6) Santos, L. O.; Dewasme, L.; Coutinho, D.; Vande Wouwer, A. Nonlinear model predictive control of fed-batch cultures of micro-organisms exhibiting over-flow metabolism: Assessment and robustness. *Comput. Chem. Eng.* **2012**, *39*, 143–151.
- (7) Dewasme, L.; Fernandes, S.; Amribt, Z.; Santos, L.; Bogaerts, P.; Vande Wouwer, A. State estimation and predictive control of fed-batch cultures of hybridoma cells. *J. Process Control* **2015**, *30*, 50–57.
- (8) Renard, F.; Vande Wouwer, A.; Valentinotti, S.; Dumur, D. A practical robust control scheme for yeast fed-batch cultures – An experimental validation. *J. Process Control* **2006**, *16*, 855–864.
- (9) Amribt, Z.; Dewasme, L.; Vande Wouwer, A.; Bogaerts, P. Optimization and robustness analysis of hybridoma cell fed-batch cultures using the overflow metabolism model. *Bioprocess Biosyst. Eng.* **2014**, *37*, 1637–1652.

- (10) Gillijns, S.; de Moor, B. Unbiased minimum-variance input and state estimation for linear discrete-time systems. *Automatica* **2007**, *43*, 111–116.
- (11) Sonnleitner, B.; Käppeli, O. Growth of *Saccharomyces cerevisiae* is controlled by its limited respiratory capacity: formulation and verification of a hypothesis. *Biotechnol. Bioeng.* **1986**, *28*, 927–937.
- (12) Gelb, A. *Applied Optimal Estimation*. MIT Press, Cambridge, 1974.
- (13) Rocha-Cózatl, E.; Moreno, J. A.; Vande Wouwer, A. Application of a continuous-discrete unknown input observer to estimation in photoplanktonic cultures, *8th IFAC Symposium on Advanced Control of Chemical Processes*, Furama Riverfront, Singapore, 10–13 July, 2012.
- (14) Bavdekar, V.; Deshpande, A.; Patwardhan, S. Identification of process and measurement noise covariance for state and parameter estimation using extended Kalman filter. *J. Process Control* **2011**, *21*, 585–601.
- (15) Zeitz, M. The extended Luenberger observer for nonlinear systems. *Systems & Control Lett.* **1987**, *9*, 149–156.